Supplemental Materials for:

CONNECTING FANO INTERFERENCE AND THE JAYNES-CUMMINGS MODEL IN CAVITY MAGNONICS

Authors

Jakob Gollwitzer[1], Lars Bocklage[1,2*], Ralf Röhlsberger[1,2,3,4,5], Guido Meier[6,2]

Affiliations

[1]Deutsches Elektronen-Synchrotron DESY, Notkestraße 85, 22607 Hamburg, Germany.

[2]The Hamburg Centre for Ultrafast Imaging, Luruper Chaussee 149, 22761 Hamburg, Germany.

[3]Institut für Optik and Quantenelektronik, Friedrich-Schiller-Universität Jena, Max-Wien-Platz 1, 07743 Jena, Germany

[4]Helmholtz Institut Jena, Fröbelstieg 3, 07743 Jena, Germany

[5]Helmholtz Centre for Heavy Ion Research (GSI), Planckstr. 1, 64291 Darmstadt, Germany

[6]Max-Planck Institute for the Structure and Dynamics of Matter, Luruper Chaussee 149, 22761 Hamburg, Germany.

*Corresponding author lars.bocklage@desy.de.

Supplementary Methods

Experimental Setup

The experimental set-up is shown in Supplementary Figure 1 and the absolute value of the reflectivity on the detuning grid is shown in Supplementary Figure 2. A fit performed using Equation (5) is shown alongside the data. The fit parameters are shown in Supplementary Table 1.

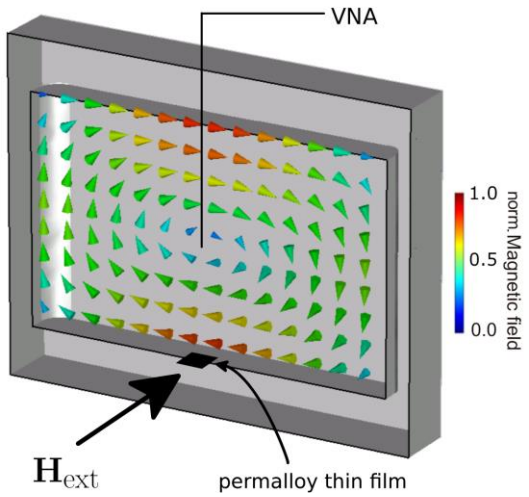

Supplementary Figure 1: Experimental setup: A permalloy film is inserted into a microwave cavity operated in the TE101 mode at its resonance frequency of $\omega_{\mathrm{res}}/2\pi \approx 3090$ MHz. The film is placed in such a way that dynamic magnetic field of the TE101 mode interacts with the magnetic dipoles of the magnetic film. The spatial magnetic field profile is calculated by a Maxwell solver and shown in the sketch. The dimensions of the cavity are 57 mm × 20 mm × 93 mm.

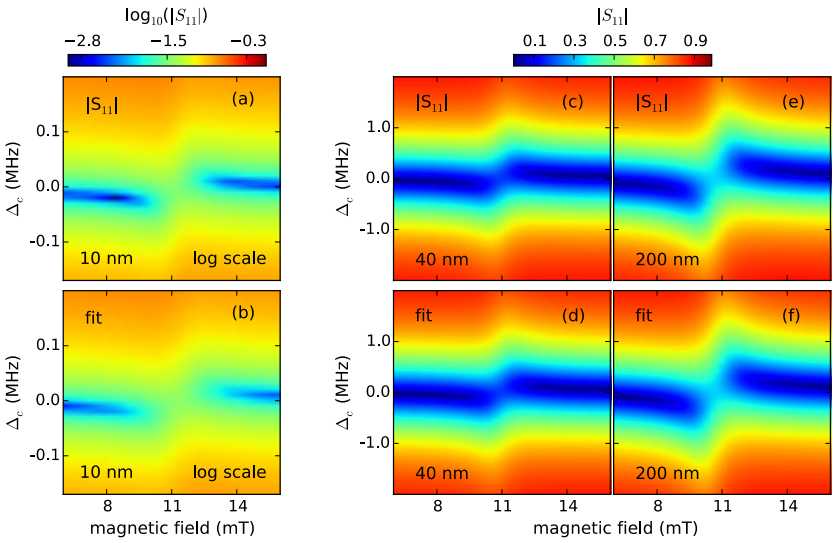

Supplementary Figure 2: $|S_{11}|$ obtained from the microwave cavity interacting with a (a) 10 nm, (c), 40 nm, and (e) 200 nm permalloy film. The Kittel mode of the permalloy film couples to the dynamic magnetic field of the cavity and induces a bend in the reflectivity spectra. As the coupling strength g increases with increasing permalloy thickness this distortion in the spectra becomes more

pronounced. Subfigures (b), (d), and (e) shows a 2D fit of the $|S_{11}|$ data with the magnitude of Equation (5).

Fit Parameter	t = 10 nm	t = 40 nm	t = 200 nm
Coupling constant $g/2\pi$	2.62 MHz	5.30 MHz	8.54 MHz
Magnonic damping $\gamma/2\pi$	169 MHz	114 MHz	129 MHz
Saturation magnetization M_s	827 kA/m	830 kA/m	902 kA/m
Anisotropy field H_k	266 A/m	529 A/m	2 A/m
Cavity damping $\kappa/2\pi$	1.12 MHz	1.13 MHz	1.13 MHz
Cavity resonance frequency $\omega_c/2\pi$	3.091 GHz	3.091 GHz	3.090 GHz
Cooperativity $C = \left(\frac{g}{\kappa}\right)\left(\frac{g}{\gamma}\right)$	0.04	0.22	0.50

Supplementary Table 1: Physical quantities extracted from the 2D fit shown in Supplementary Figure 2. The trend of the coupling constant increasing as a function of the square root of the number of spins in the cavity is evident. The last row shows the cooperativity C.

Auxiliary Calculations

Steps to rewrite the square of the absolute value of the reflectivity (Equation (5)) in a generalized Fano form (Equation (6)) include:

$$r = 1 + \frac{\kappa}{\mathrm{i}\Delta_c + \kappa + \frac{g^2}{\mathrm{i}\Delta_m + \gamma}} = -1 + \frac{(\varepsilon+\mathrm{i})\mathrm{i}}{\left(-\frac{\Delta_c}{\kappa}+\mathrm{i}\right)(\varepsilon+\mathrm{i}) - C} = \frac{\left(\varepsilon+\mathrm{i}+C\frac{\kappa}{\Delta_c}\right)\frac{\Delta_c}{\kappa}}{(\varepsilon+i)\left(-\frac{\Delta_c}{\kappa}+\mathrm{i}\right)-C} \quad (1)$$

The quantity of interest is $|r|^2$ which may be written as

$$|r|^2 = \frac{\left(\frac{\Delta_c}{\kappa}\right)^2}{\left(\frac{\Delta_c}{\kappa}\right)^2+1} \frac{\left|\varepsilon+\mathrm{i}+C\frac{\kappa}{\Delta_c}\right|^2}{\varepsilon^2+1+\frac{2C\left(\frac{\varepsilon\Delta_c}{\kappa}+1\right)+C^2}{\left(\frac{\Delta_c}{\kappa}\right)^2+1}} = \sigma_0\left(\frac{(\varepsilon+\mathrm{Re}(\tilde{q}))^2}{\varepsilon^2+\eta^2} + \frac{\mathrm{Im}(\tilde{q})^2}{\varepsilon^2+\eta^2}\right) \quad (2)$$

with the definitions of σ_0, η, $\tilde{q}$ and ε given in the text. The term $\eta = \sqrt{1+f}$ is given by

$$f(\varepsilon, \Delta_c, C) = \left(2C\left(\frac{\Delta_c}{\kappa}\varepsilon + 1\right) + C^2\right) / \left(\frac{{\Delta_c}^2}{\kappa^2} + 1\right) \quad (3)$$

which scales quadratically with the cooperativity C and linearly with ε. For low cooperativities $\eta^2 \approx 1$. The value of η^2 on the cavity and magnon detuning grid is shown in Supplementary Figure 3 for the three thickness cases of the permalloy film investigated in this study. Only for the case t = 10 nm does η^2 not deviate strongly from unity so that the Fano interference picture remains valid.

Line shapes at large cavity detunings

The role of the second term connected to the imaginary part of $\tilde{q}$ in changing the Fano lineshape becomes significant when the cavity detuning Δ_c increases beyond $\Delta_c > \kappa C$ (see Supplementary Figure 1(c) and (e)). As Δ_c increases, the real part $\mathrm{Re}(\tilde{q})$ becomes small and the imaginary part causes $|r|^2$ to become the division between two parabolas $|r|^2 \approx \sigma_0(\varepsilon^2+1)/(\varepsilon^2+1+f)$. They dependent on the dimensionless magnon detuning ε. In this regime the lineshape is dominated by the additional term f which depends inversely on Δ_c so that the divided parabolas are slightly shifted in ε to one another. This leads to a dip in the reflectivity around $\varepsilon = 0$. The amplitude of the dip is determined by the resonant cross section σ_0 and by the magnitude of f. The dependence of f on Δ_c as shown in Equation (3) indicates that as $\Delta_c \to \infty$, the offset between the divided parabolas decreases to zero and the amplitude of the dips becomes invisible.

The Fano Phase Picture

To rewrite the first term in Equation (6) into the Fano interference picture of Equation (7) one may write

$$\frac{|\varepsilon+\mathrm{Re}(\tilde{q})|^2}{\varepsilon^2+\eta^2} = \frac{|\varepsilon+\mathrm{i}+\mathrm{Re}(\tilde{q})-\mathrm{i}|^2}{|\varepsilon+\mathrm{i}\eta|^2} = \left|1+\frac{\mathrm{Re}(\tilde{q})-\mathrm{i}}{\varepsilon+\mathrm{i}\eta}\right|^2 \tag{5}$$

Identifying the complex numbers $\mathrm{Re}(\tilde{q})-\mathrm{i}$ and $1/(\varepsilon+\mathrm{i}\eta)$ and writing them in terms of magnitudes and phases via standard complex analysis yields

$$\frac{|\varepsilon+\mathrm{Re}(\tilde{q})|^2}{\varepsilon^2+\eta^2} = \left|e^{\mathrm{i}\varphi_c} + \frac{|\mathrm{Re}(\tilde{q})-\mathrm{i}\eta|}{\sqrt{\varepsilon^2+\eta^2}}e^{\mathrm{i}\varphi_m}\right|^2 \tag{6}$$

with $\varphi_c = -\arg(\mathrm{Re}(\tilde{q})-\mathrm{i}\eta)$ and $\varphi_m = \arg(\varepsilon-\mathrm{i}\eta)$ as in Equation (7).

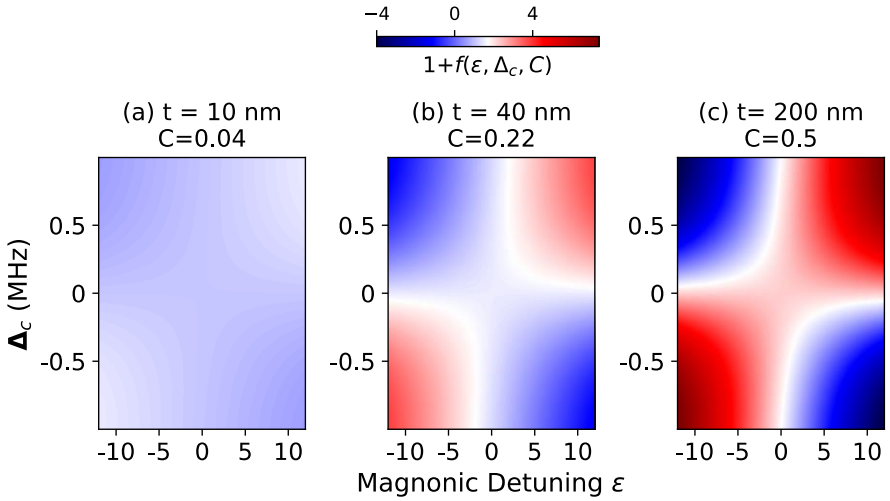

Supplementary Figure 3. The value of $\eta^2 = 1 + f$ on the 2D detuning grid for the case of a (a) 10 nm, (b) 40 nm, and (c) 200 nm thick permalloy film. Parameters obtained by the fit are shown in Supplementary Table 1. For the 10 nm film, a maximum deviation from unity of η^2 of approximately 0.3 is observed and ηremains real on all points on the grid. Hence, the generalized Fano form (Equation (6)) may be written in the Fano interference form (Equation (7)). As the thickness and cooperativity increases ((b) and (c)), the deviation of η^2 from unity on the detuning grid becomes more pronounced. On sections of the detuning grid on which $\eta^2 < 0$, η becomes purely imaginary so that the generalized Fano interference picture (Equation (7)) ceases to apply.

Difference in transmission and reflection spectra

The transmission spectrum at critical coupling is given by [9]

$$t = \frac{\kappa}{\mathrm{i}\Delta_\mathrm{c} + \kappa + \frac{g^2}{\mathrm{i}\Delta_\mathrm{m} + \gamma}}. \tag{7}$$

Following the same calculations as for the reflectivity one obtains

$$|t|^2 = \sigma_0^\mathrm{t}\left(\frac{(\varepsilon + \mathrm{Re}(\tilde{q}))^2}{\varepsilon^2 + \eta^2} + \frac{\mathrm{Im}(\tilde{q})^2}{\varepsilon^2 + \eta^2}\right) \tag{8}$$

with $\mathrm{Re}(\tilde{q}) = 0$ and $\sigma_0^\mathrm{t} = (1 + \Delta_\mathrm{c}^2/\kappa^2)^{-1}$. A real part of zero of the complex asymmetry parameter leads to a constant cavity phase of $\pi/2$. Comparing the relation for the reflectivity $\mathrm{Re}(\tilde{q}) = C\,\kappa/\Delta_\mathrm{c}$ with the vanishing real part in transmission, indicates that reflectivity and transmission features are similar for large cavity detuning and determined mainly by η^2.
In the interferometric picture of the Fano resonance the changes of the phases in the different channels are what determines the lineshape. Therefore, to understand this difference in the dependence of $\mathrm{Re}(\tilde{q})$ on the cavity detuning one has to reveal the phase relation inside the cavity. From the input-output formalism the transmission and reflection coefficients are given by [9]

$$t = \frac{d_\mathrm{out}(t)}{c_\mathrm{in}(t)} \qquad \text{and} \qquad r = \frac{c_\mathrm{out}(t)}{c_\mathrm{in}(t)} \tag{9}$$

that relate the incoming and outgoing waves at the ports of the cavity; port 1 ($c_\mathrm{in}, c_\mathrm{out}$) and port 2 ($d_\mathrm{out}$). Those relations lead to Equations (5) and (7). These relations implicitly contain the phase information at the ports. The wave inside the cavity $c(t)$ is described by

$$\frac{c(t)}{c_\mathrm{in}(t)} = \frac{\kappa}{\mathrm{i}\Delta_\mathrm{c} + \kappa + \frac{g^2}{\mathrm{i}\Delta_\mathrm{m} + \gamma}} \tag{10}$$

which is the same as the one for the transmission. Thus, the phase inside the cavity and the one measured at the transmission port are always identical. The wave inside the cavity drives the magnon inductively whose phase is related to this excitation (the phase shift of $\pi/2$). No dependence on the detuning can be expected for the transmission because the phase inside the cavity and at the transmission port are always the same and the magnon phase changes with respect to this common phase. This situation however changes for the reflectivity.
In Supplementary Figure 4(a), we plot the phases of transmission and reflection of an empty cavity ($g = 0$). The magnitude of the phase difference is constant and the phase experiences a phase jump of π at zero detuning. Thus, for the empty cavity reflectivity and transmission have a fixed phase relation with detuning. The situation changes when the cavity is coupled to the magnon mode, see Supplementary Figure 4(b). The phase of the transmission changes only slightly with respect to the

empty cavity. It's noteworthy that the photon phase inside the cavity, which drives the magnon and determines the magnons phase, is the same as for the transmission here as well. The phase of the reflectivity is changed considerably when coupled to the magnon. In the interferometric picture, the background phase of the cavity thus changes with respect to the magnon (or transmission) phase. The difference of the phases reveals the same behavior as the cavity phase of the reflection in the Fano model $\varphi_c = -\arg(\mathrm{Re}(\tilde{q}) - \mathrm{i}\eta)$ with the additional phase jump. The phase difference has been fit to $\varphi = -\arg(C\,\kappa/\Delta_c - \mathrm{i}) + \alpha$, where C and α are free parameters. The fit cooperativity $C = 0.22$ is exactly the one derived from the Fano fit for the 40 nm film (see Fig. 2 in the main text). The phase jump of π is fit by $\alpha(\Delta_c)$. The parameters η has been omitted as it is $\eta \approx 1$ at zero magnon detuning. Only at large cavity detuning the empty cavity phase difference is restored, which also indicates that at large detuning the background phases of transmission and reflection have a fixed relation in the Fano formula.

The difference in the real part of the asymmetry parameter in the transmission and reflection is thus given by a relative phase change of the reflected signal with respect to the phase inside the cavity. For the transmission both cavity phase and transmission phase are equal and no dependence on the detuning is found. For the reflectivity the phase changes with respect to the cavity phase and manifests as a detuning dependent $\mathrm{Re}(\tilde{q})$.

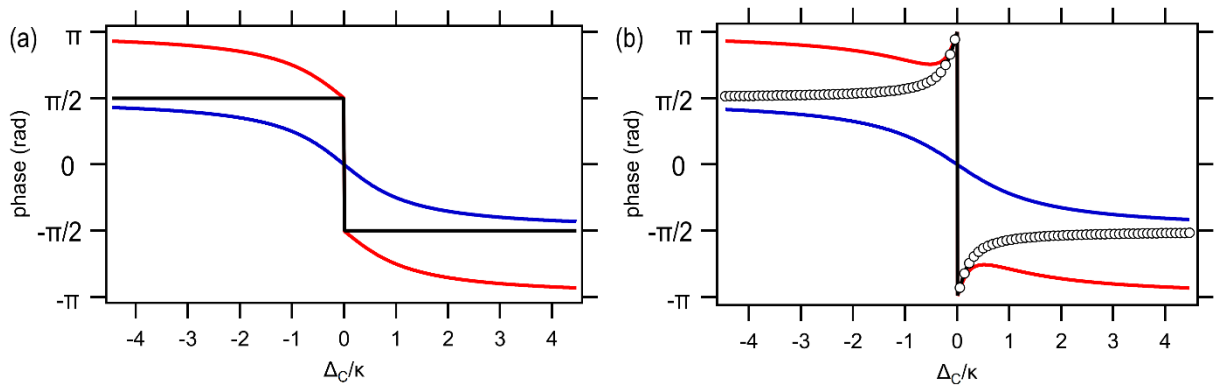

Supplementary Figure 4. Phases of transmission (blue) and reflection (red) of the cavity. (a) shows the phases for an empty cavity. Their phase difference $d = r - t$ is shown in black and reveals a constant absolute value with a phase jump of π at zero detuning. (b) Phases for a cavity with a magnetic film inserted at zero magnon detuning. The coupling parameters are the one of the 40 nm film. The phase for transmission is only slightly changed while the phase in the reflectivity shows considerable changes when approaching small detuning. Dotted curve is a fit to the phase difference (see text).